# Electronic Transitions at Si(111)/SiO$_2$ and Si(111)/Si$_3$N$_4$ Interfaces Studied by Optical Second-Harmonic Spectroscopy

C. Meyer, G. Lüpke, U. Emmerichs, F. Wolter, and H. Kurz
*Institute of Semiconductor Electronics II, Rheinisch-Westfälische Technische Hochschule, D-52056 Aachen, Germany*

C. H. Bjorkman
*Research Center for Integrated Systems, Hiroshima University, 1-4-2 Kagamiyama, Higashi-Hiroshima 724, Japan*

G. Lucovsky
*Departments of Physics, Material Science and Engineering, and Electrical and Computer Engineering,*
*North Carolina State University, Raleigh, North Carolina 27695-8202*

(Received 15 December 1994)

The existence of both strain and disorder at the interface of thermally grown SiO$_2$ or plasma-deposited Si$_3$N$_4$ films on vicinal Si(111) was ascertained unambiguously by frequency, polarization, and crystal orientation dependent studies of optical second-harmonic generation. The strain was seen to cause a redshift of 40 and 70 meV of the interband critical points $E_0'$ and $E_1$ compared with the bulk silicon values. The disorder is observed by the perturbation of states out of the silicon bulk bands into the gap. Both at terraces and at steps, the density of these charge traps is found to be considerably reduced after rapid thermal annealing.

PACS numbers: 73.20.–r, 42.65.Ky, 68.35.Bs

Strain and order or disorder at the heterointerfaces in semiconductors significantly affect the electrical device characteristics [1–4]. For instance, the disorder of Si/SiO$_2$ interfaces has been reported to degrade electron mobility and increase oxide and interface charge trap densities [1,2]. On the other hand, lower strain-induced band-gap modifications and improved transport properties of the carriers are the main reasons to form various heterostructure devices on Si. However, the Si band-structure modulation due to the strain along the Si/SiO$_2$ interface has not been studied well, although it is the major issue of the Si/Ge interface and III-V compound interfaces.

Second-order nonlinear optical probes are well suited for studying interfaces buried between centrosymmetric media as they possess long penetration depths and intrinsic interface specificity. Recently they have been used with considerable success to probe solid/solid interfaces [5–13]. Several studies on vicinal Si(111)/SiO$_2$ and Si(100)/SiO$_2$ interfaces have employed the tensorial characteristic of second-harmonic generation (SHG) to examine the chemical bonding arrangements at atomic-scale steps [9,12] and kink sites [13]. However, very few SHG studies have taken advantage of the energy resolution available from optical probes. Heinz and co-workers carried out frequency-dependent three-wave mixing experiments on CaF$_2$/Si(111) interfaces [5], in which they detected an interfacial band gap with an energy separation well within the band gap of CaF$_2$. Furthermore, Daum *et al.* observed in their sum-frequency generation and SHG spectroscopy experiments on clean and oxidized silicon interfaces a direct band-gap transition in a few monolayer thin silicon region at the Si-SiO$_2$ interface with increased interlayer spacings [11]. However, despite this auspicious beginning, we have barely begun to develop a microscopic understanding of the role played by interfacial excitations in affecting nonlinear optical phenomena. The primary reasons for this are the complicated form of the nonlinear response functions and the greater sensitivity of the susceptibility tensors to the details of the energy band structure and wave functions of the electrons.

In this study we demonstrate the application of SHG spectroscopy to directly identify the physical origin and nature of various electronic transitions at Si(111)/SiO$_2$ and Si(111)/Si$_3$N$_4$ interfaces. Evidence for band-gap narrowing at the $\Gamma$ point of the Si(111) interface Brillouin zone (BZ) is given for the first time. The occurrence of two SH resonances shifted to lower energies compared with the lowest direct band-gap transitions in silicon indicates an expansion of Si-Si bonds oriented vertically and laterally to the interface normal. In addition, we show that the nonlinear optical susceptibility of the interlayer includes the effect of "mild disorder" at the interface. The term mild disorder implies that the bonding between Si atoms is maintained but that the individual bonds are bent and stretched in different ways, thereby causing the perturbation of states out of the Si bulk bands into the gap [14]. The present measurements are the first to demonstrate directly the reduction of these gap states after rapid thermal annealing of thermally grown Si(111)/SiO$_2$ interfaces.

In our experiments we used optically flat standard silicon wafers cut with a small offset angle $\alpha \simeq 4.5° \pm 0.5°$ between optical surface normal and [111] toward the $[11\bar{2}]$ direction to get a regular step structure. On these wafers two different interfaces were prepared: (i) thermal oxides (thickness $\simeq$ 60 nm) were grown at 850 °C in a dry oxygen ambient; (ii) nitride films (thickness $\simeq$ 30 nm) were deposited via a remote plasma-enhanced chemical vapor deposition.

For SH dispersion measurements, a beam of 30 mW average power consisting of 100 fs pulses at 76 MHz generated by a mode-locked titanium:sapphire laser was focused on the sample to a 20-$\mu$m-diam spot at a 45° angle of incidence. In all experiments, we detected the $p$-polarized SH response $I^{(2\omega)}_{g,p}$ produced by excitation with a $g$-polarized fundamental field $E^{(\omega)}_g$, where $g = s$ or $p$. $I^{(2\omega)}_{g,p}$ depends on the sample azimuthal angle $\phi$ as given by

$$I^{(2\omega)}_{g,p}(\phi) = |\chi^{(2)}_{\mathrm{eff}} E^{(\omega)}_g E^{(\omega)}_g|^2 = |a_0^{g,p} + a_1^{g,p}\cos(\phi) + a_3^{g,p}\cos(3\phi)|^2, \quad (1)$$

for a surface with $C_{1v}$ symmetry [15]. The $\chi^{(2)}_{\mathrm{eff}}$ is the effective second-order susceptibility, and $a_i^{g,p}$ ($i = 0$, 1, and 3) are linear combinations of $\chi^{(2)}_{ijk}$ multiplied by angle-of-incidence-dependent Fresnel factors. Using Eq. (1) to fit the azimuthal dependence of the SH intensity taken at different SH wavelengths between 350 and 400 nm we have deduced the frequency dependence of $|a_0^{g,p}|^2$, $|a_1^{g,p}|^2$, and $|a_3^{g,p}|^2$. The results are summarized in Figs. 1(a)–1(c) as a function of the SH photon energy.

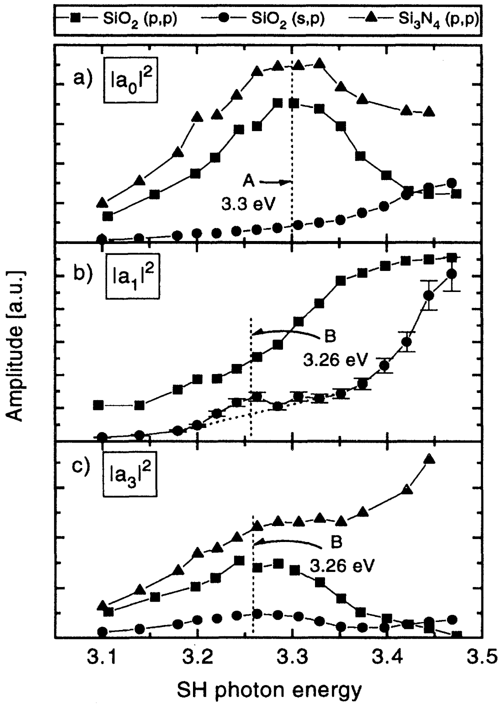

FIG. 1. SH Fourier coefficients as a function of SH photon energy: (a) the isotropic coefficient $|a_0^{g,p}|^2$, (b) the step-induced onefold coefficient $|a_1^{g,p}|^2$, and (c) the threefold coefficient $|a_3^{g,p}|^2$. The squares and triangles represent $p$-polarized incident light, the circles represent $s$-polarized incident light. The curves are not to scale.

A strong peak $A$ centered at 3.3 eV is clearly evident in Fig. 1(a) for $p$-polarized incident light. In contrast, $|a_0^{s,p}|^2$ varies only slowly with SH photon energy. Since linear optical effects and the isotropic bulk electric quadrupole contribution ($\gamma$) contribute in the same way to both $a_0^{p,p}$ and $a_0^{s,p}$ [15], they can be ruled out as the reason for the observed SH resonance. Thus, the strongest candidates for the peak at $2\hbar\omega = 3.3$ eV are the isotropic electric dipolar $\chi^{(2)}$ tensor elements. Furthermore, in Fig. 1(c) a maximum at $B$ appears in the $|a_3^{s,p}|^2$ and $|a_3^{p,p}|^2$ spectra at a slightly lower energy of 3.26 eV with respect to peak $A$. We are able to determine which contribution leads to the peak at 3.26 eV by investigating the frequency dependence of the step-induced onefold coefficients $a_1^{s,p}$ and $a_1^{p,p}$, shown in Fig. 1(b). As one can infer from Fig. 1(b), $|a_1^{s,p}|^2$ exhibits a small peak at 3.26 eV, whereas no peak is visible in the spectra of $|a_1^{p,p}|^2$. Since both $a_1^{g,p}$ and $a_3^{g,p}$ contain contributions from the anisotropic bulk response $\zeta$, but contain contributions from different $\chi^{(2)}$ tensor elements, we can assign the peak at 3.26 eV to a resonance in the anisotropic electric dipolar $\chi^{(2)}$ tensor elements [15]. Separate sum-frequency experiments confirmed that both peaks ($A$ and $B$) are two-photon resonances.

We now consider the possible transitions which can contribute to the observed SH frequency dependence. From Fig. 1 it is obvious that the reason for the resonances at 3.26 and 3.3 eV in our spectra must be the same for the Si(111)/SiO$_2$ and Si(111)/Si$_3$N$_4$ interfaces. Previous SH experiments have shown that the resonance at 3.3 eV occurs on clean Si(100):2 × 1 and Si(111):7 × 7 as well as on oxidized surfaces [11]. The energetic position of both SH resonances (3.26 and 3.3 eV) matches to the lowest direct energy gaps in silicon. The lowest direct energy gap, labeled $E_0'$ (3.3 eV) and located at the $\Gamma$ point, is nearly degenerate with the $E_1$ (3.37 eV) transitions, which take place along the $\Lambda$ direction of the BZ [16]. Thus we assign the resonant enhancement in our spectra to direct transitions between states close to the valence and conduction band edges at the $\Gamma$ point of the Si(111) interface BZ.

To confirm this assignment we now focus on the polarization selection rules for possible electronic transitions. Each independent tensor element of $\chi^{(2)}$ will, in general, manifest different resonances [5]. The selection rules which define the necessary orientation of the incident light polarization with respect to the crystal axes can be derived in a straightforward manner by considering the symmetry of states at various critical points of the silicon BZ in coordinate space. Let the $x$-$y$ plane be fixed to the crystal surface, with the $x$ axis parallel to the projection of the $[11\bar{2}]$ axis on the surface, and the $z$ axis normal to the crystal surface, as indicated in Fig. 2.

Peak $A$ at 3.3 eV can be assigned to $\chi_{zzz}$, since peak $A$ is present in the spectral dependence of $a_0^{p,p}$ containing contributions from $\chi_{zzz}$, $\chi_{zxx}$, and $\chi_{xzx}$, and is missing in the spectra of $a_0^{s,p}$ arising from $\chi_{zyy} = \chi_{zxx}$ [15]. This assign-

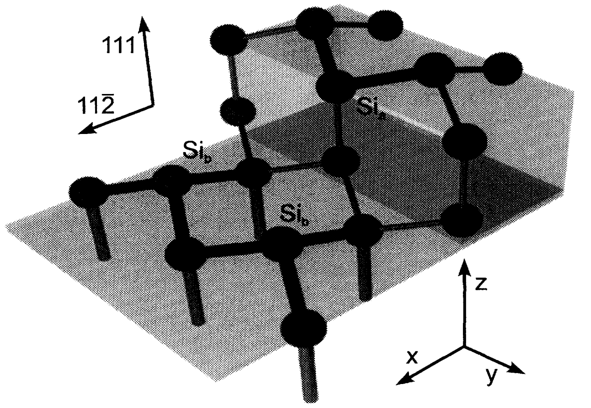

FIG. 2. Stick-and-ball model of the local bonding geometry between the first and second Si atomic layers along the [11$\bar{2}$] step edge.

ment is in agreement with the observation made by Daum *et al.* [11]. Since the lowest conduction band state has $\Lambda_1$ symmetry (like an $s$ or $p_z$ orbital) along the $\Lambda$ direction, only $\chi_{zzz}$ (peak $A$ at 3.3 eV) will exhibit resonances (in the dipole approximation) for transitions at the $E_1$ critical point [5,16]. Furthermore, peak $B$ at 3.26 eV in the spectra of $a_3^{s,p}$ and $a_3^{p,p}$ can be related to a resonance in the threefold component of $\chi_{xxx}$ and $\chi_{xyy}$ which reflects the $C_{3v}$ symmetry of the Si(111) terraces [15]. The $\chi_{xxx}$ and $\chi_{xyy}$ tensor elements include contributions from states of $\Lambda_3$ symmetry ($p_x$, $p_y$ character) corresponding to the $C_{3v}$ point group symmetry of the states involved in the $E_0'$ transition at the $\Gamma$ point [16]. Thus, the strongest candidates for the resonances at $2\hbar\omega = 3.26$ and 3.3 eV are electronic transitions at the $E_0'$ and $E_1$ direct band gaps in silicon. To our knowledge this is the first time that the $E_0'$ and $E_1$ critical points in silicon could be completely separated by the polarization selection rules in an optical experiment.

The fact that peaks $A$ and $B$ are shifted by 40 and 70 meV to lower photon energy compared with the bulk values of $E_0'$ and $E_1$, respectively, indicates the presence of a strained Si interlayer [11,17,18]. It has been established that uniaxial stress causes a splitting and shift of the $E_1$ transition in bulk silicon [19]. For the Si/SiO$_2$ system in our study, the splittings may be too small to be experimentally observed. Therefore, the redshift is due to the interlayer being strongly influenced by the hydrostatic component of the strain [17,18]. The hydrostatic pressure can be calculated using the value of the redshift and the elastic constants and potential deformation of Si [18]. For our samples, a redshift of 70 meV corresponds to a tensile hydrostatic pressure of $\sim 15 \times 10^9$ dyn/cm$^2$, or a relative change in volume of $\sim 1\%$, which is in excellent agreement with the data obtained by Fitch, Bjorkman, and Lucovsky from their photoreflectance measurements on the samples grown at the same temperature (850 °C) [18]. Regarding the extent of the strain, the above authors' estimate of the thickness is 10 nm [18], in contrast to a recent spectroscopic ellipsometry study showing that the extent of the strained silicon region is $\sim 1.5$ nm into the substrate [17]. The existence of a few monolayers of strained Si at the interface appears to be supported by the occurrence of a small peak at 3.26 eV in the spectra of the step-induced coefficient $a_1^{s,p}$ [see Fig. 1(b)] containing contributions from $\chi_{xyy}$ [15]. As indicated in Fig. 2, Si-Si bonds at the [11$\bar{2}$] step atoms, Si$_a$, are preferentially aligned along the $y$ axis, thus contributing mainly to $\chi_{xyy}$. On the other hand, the onefold component of $\chi_{xxx}$ contributing to $a_1^{p,p}$ exhibits no resonance features [see Fig. 1(b)]. This is consistent with the fact that the Si$_a$ bond pointing preferentially toward the direction of the $x$ axis is mainly terminated by an oxygen or nitrogen atom depending on the interface, and thus its resonance energy is shifted toward higher energies [10,20]. On the terraces, however, all three backbonds of the Si$_b$ atom are terminated by a silicon atom, and can contribute to both $a_3^{s,p}$ and $a_3^{p,p}$, as demonstrated in Fig. 1.

We next turn our attention to interface states due to weakened or bent Si-Si bonds at the interface. In general, such states split off from bulk bands at critical points, and transitions between these states and bulk states with a wave vector similar to that of the critical point nearest to the interface state will be enhanced [14]. Thus, to check the presence of these metastable states at the interface, we have taken SH spectra of $|a_i^{p,p}|^2$ from thermally grown Si(111)/SiO$_2$ interfaces subjected to rapid thermal annealing (RTA) at different temperatures from 900 to 1100 °C for 100 s in a dry argon atmosphere. Annealing of the Si/SiO$_2$ interface is a standard silicon technology process to reduce the built-in stress at the interface and the density of interface charge traps [10].

The results are presented in Fig. 3. In the spectra of $|a_i^{p,p}|^2$ the amplitude and energetic position of both resonances (peaks $A$ and $B$) do not significantly change with increasing annealing temperature, whereas the background with increasing slope to the high-energy side decreases dramatically above 950 °C. The former observation can be explained by the high intrinsic stress of $(4.6 \pm 0.5) \times 10^9$ dyn/cm$^2$ at the Si/SiO$_2$ interface, primarily due to the mismatch between the molar volumes of Si and SiO$_2$, subject to constraints imposed by the chemical bonding at the interface [18]. The latter observation demonstrates that part of the SH response in our spectra arises from transitions between valence/conduction band states and interface states due to disordered Si-Si bonds. The density of these states can be considerably reduced by a RTA step, leaving behind a residual, U-shaped distribution of interface gap states with steeply increasing tails toward the bulk valence and conduction band edges [10]. The correlation between the density of interface charge traps and the SH response of chemically modified vicinal Si(111) surfaces has been demonstrated recently by Emmerichs *et al.* [12]. They observed that after annealing at 900 °C the density of interface traps $D_{\mathrm{IT}}$ is decreased, supported by comple-

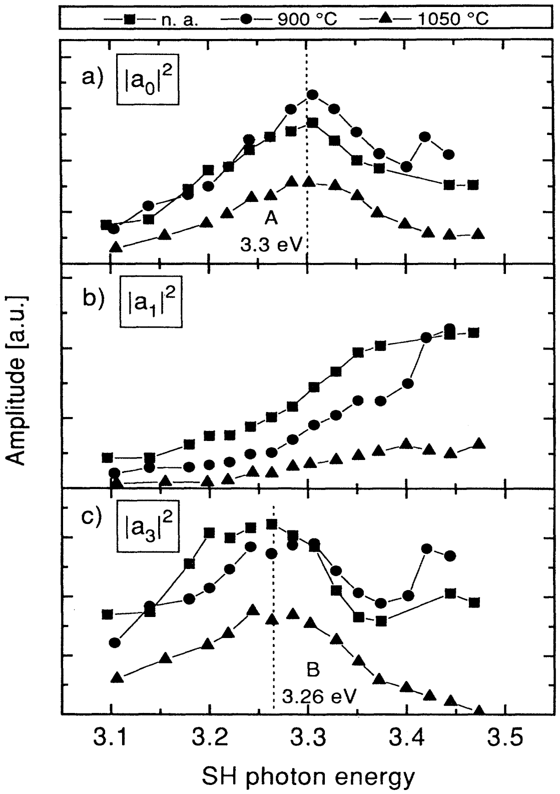

FIG. 3. The dependence of $|a_0^{p,p}|^2$, $|a_1^{p,p}|^2$, and $|a_3^{p,p}|^2$ (a)–(c) on SH photon energy obtained from a thermally grown Si(111)/SiO$_2$ interface as grown (squares), and after annealing to 900 °C (circles) and 1050 °C (triangles).

mentary $C$-$V$ measurements [10]. Thus, the overall background reduction in our spectra with increasing annealing temperature can be explained by a rearrangement of atomic bonds at the interface into more favorable positions, particularly for the step-induced $a_1^{p,p}$ component. This leads us to the conclusion that the Si/SiO$_2$ interface region consists of a few monolayer thin strained silicon layer underneath a "mild-disordered" layer. Although the underlying Si near the interface is strained, the structural perfection still remains high, as displayed by the sharpness of $E_0'$ and $E_1$ transitions.

In summary, we have utilized second-harmonic spectroscopy to study electronic transitions at Si(111)/SiO$_2$ and Si(111)/Si$_3$N$_4$ interfaces. A strained Si interlayer was seen to cause a redshift of 40 and 70 meV of the Si interband critical points $E_0'$ and $E_1$. A detailed analysis of the SH spectra with respect to polarization selection rules, along with the symmetry elements, have enabled us to make a stronger and more precise assignment of the location and origin of electronic trap states at the interface. Both at terraces and at steps, the density of these gap states is found to be considerably reduced after rapid thermal annealing. Similar studies can be performed on vicinal Si(100) surfaces, on which interfacial anisotropic contributions to SHG up to threefold in symmetry are permitted, enabling electronic transitions present to be investigated.

We would like to thank P. Krüger for fruitful discussions on electronic transitions at silicon surfaces. The research presented in this paper is jointly supported by the Deutsche Forschungsgemeinschaft, the National Science Foundation, the Office of Naval Research, and by a specific scientific collaboration between the states of Nordrhein-Westfalen and North Carolina.

[1] R. People, IEEE Trans. Quantum Electron. **22**, 1696 (1986).
[2] G.C. Osbourn, IEEE Trans. Quantum Electron. **22**, 1677 (1986).
[3] T. Ohmi, K. Kotani, A. Teramot, and M. Miyashita, IEEE Electron Device Lett. **12**, 652 (1991).
[4] P.O. Hahn and M. Henzler, J. Vac. Sci. Technol. A **2**, 574 (1984).
[5] T.F. Heinz, F.J. Himpsel, E. Palange, and E. Burstein, Phys. Rev. Lett. **63**, 644 (1989).
[6] S.V. Govorkov *et al.,* J. Opt. Soc. Am. B **6**, 1117 (1989).
[7] L.L. Kulyuk, D.A. Shutov, and E.E. Strumban, J. Opt. Soc. Am. B **8**, 1766 (1991).
[8] M.S. Yeganeh, J. Qi, A.G. Yodh, and M.C. Tamargo, Phys. Rev. Lett. **69**, 3579 (1992).
[9] G. Lüpke, D.J. Bottomley, and H.M. v. Driel, Phys. Rev. B **47**, 10 389 (1993).
[10] C.H. Bjorkman *et al.,* J. Vac. Sci. Technol. B **11**, 1521 (1993).
[11] W. Daum, H.-J. Krause, U. Reichel, and H. Ibach, Phys. Rev. Lett. **71**, 1234 (1993).
[12] U. Emmerichs *et al.,* Phys. Rev. B **50**, 5506 (1994).
[13] G. Lüpke, C. Meyer, U. Emmerichs, F. Wolter, and H. Kurz, Phys. Rev. B **50**, 17 292 (1994).
[14] C. Svenson, in *The Si-SiO2 System,* edited by P. Balk, Materials Science Monographs Vol. 32 (Elsevier, New York, 1988), Chap. 5, p. 221.
[15] G. Lüpke, D.J. Bottomley, and H.M. van Driel, J. Opt. Soc. Am. B **11**, 35 (1994).
[16] P. Lautenschlager, M. Garriga, L. Viña, and M. Cardona, Phys. Rev. B **36**, 4821 (1987).
[17] N.V. Nguyen, D. Chandler-Horowitz, P.M. Amirtharaj, and J.G. Pellegrino, Appl. Phys. Lett. **64**, 2688 (1994).
[18] J.T. Fitch, C.H. Bjorkman, and G. Lucovsky, J. Vac. Sci. Technol. B **7**, 775 (1989).
[19] F.H. Pollak and G.W. Rubloff, Phys. Rev. Lett. **29**, 789 (1972).
[20] S. Tokumitsu *et al.,* Surf. Sci. **317**, 143 (1994).

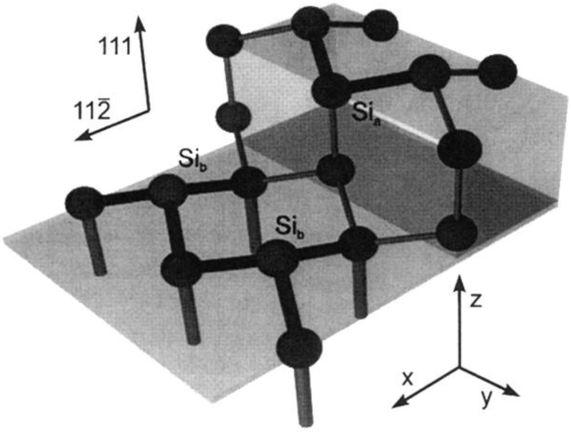

FIG. 2. Stick-and-ball model of the local bonding geometry between the first and second Si atomic layers along the $[11\bar{2}]$ step edge.